ATTRIBUTE OF WAVELET EXTRACTION FOR SEISMIC-TO-WELL TIE ANALYSIS OF ETA (η) FIELD, SOUTHERN NIGER DELTA

ISSN: 2141 – 3290
www.wojast.com

ATAT, J. G., ESSIEN, K. E, AND EKPO, S. S.
Department of Physics, University of Uyo, Nigeria
josephatat@uniuyo.edu.ng; kantville@gmail.com; sundayekpo@uniuyo.edu.ng

ABSTRACT

We used seismic nad well-log data from two wells (G and H) location in the Eta (η) field of Niger Delta basin to investigate the attribute of wavelet extraction on the record interpretation of the field. The software used is Hampson Russell. We considered both the deterministic and statistical approahes of wavelet extraction. Result obtained indicates that statistically extracted wavelet used for well correlation resulting in cross correlation plot of time shift -84ms up with correlation coefficient of <51% and -69ms up with correlation coefficient of <18%. When re-extracted, the well option wavelet used for well correlation leads to a plot of time shift 0ms and correlation coefficient of >60% for well G; 53% for well H with the same time window of the wavelet estimation. Seismic wavelets vary with time which seriously affects the accuracy of seismic exploration. The wavelet spectrum is more effective and feasible as it improves the results of the two wells.

INTRODUCTION

The vertical resolution of seismic data is significantly affected by time-varying seismic wavelets; the phase extraction is important for the precise wavelet extraction. In real seismic data, seismic wavelets are spread and absorbed by the subsurface medium as they propagate; subsequently the energy is attenuated resulting in the phase alteration of the wavelets. Consequently, seismic wavelets vary with time which seriously affects the accurateness of seismic exploration (Margrave and Lamoureux, 2001).

Seismic wavelet assessment is essential part of seismic data processing and analysis. The procedures for seismic wavelet extraction may be grouped as deterministic and statistical. Relating the deterministic spectral coherence approach and statistical skewness attribute technique, the amplitude and phase of the time-varying wavelet are obtained distinctly. There is no assumption on the wavelet's time-independent nature or the phase characteristic. Phase corrections are applied using time-varying phase rotation. Otherwise, amplitude and phase deconvolution can be accomplished to improve the resolution and support a satisfactory reservoir description. Both synthetic and real data instances may be demonstrated. Synthetic verifies its feasibility; real data validates the ability to evaluate the time-varying property of wavelets (Wei *et al*., 2017). Deterministic has to do with employing physical theories of wave propagation comprising the solution of integral and differential equations where boundary and initial conditions are satisfied. Statistical technique or method employs statistical theories of time series to have the expression of the dynamics as a statistical fact (Robinson and Treitel, 2000).

Weglein and Secrest (1990) suggested a wavelet estimation technique from wave theory (the total wavelet comprising the phase and source-array pattern). The theory allows an acoustic (marine) or elastic (land) wavelets to be consistent with the earth model when used for data processing. Tan (1999) proposed a technique to assess the wavelet spectrum with respect to the acoustic wave equation. His approach does not involve statistical assumption; the most significant are whiteness of the earth's reflectivity series and the minimum-phase character of wavelet. Geo *et al*., 2017 considered the statistical approach which is based on the convolution model of a seismic trace. A stage in seismic processing for the shape of the wavelet (also called the embedded wavelet) which may also be extracted via autocorrelation of the seismic trace, by assuming the phase of the wavelet in any case (Schlumberger, 2020).

In marine seismic exploration, ghost wave and bubble effect really decrease the vertical resolution and interpretation accuracy. The far-field wavelets like source wavelet, ghost wave and bubble effect recorded by the Vertical Cable System (VCS) is extracted. Filters are designed by means of the extracted far-field wavelet to remove ghost wave, bubble effect and source wavelet. These designed filters are applied to the seismic data of VCS. The findings indicate that this technique can exclude ghost wave, bubble effect and source wavelet effectively leading to a much better and clear vertical resolution of the seismic data (Wang *et al*., 2017).

Two key parameters of seismic inversion are low frequency and wavelet (band pass filter imposed by seismic acquisition). The low frequency section is results from well data; high frequency from seismic data. For better interpretation of seismic data, seismic inversion increases data efficiency and quality to better rock properties assessment. It eliminates the influence of the wavelet within the seismic bandwidth. Seismic inversion method requires seismic data and wavelet estimated from the data (Atat *et al*., 2020).

GEOLOGY

The Niger Delta is located (Klett *et al*., (1997) between latitudes 3^0N and 6^0N; longitudes 5^0E and 8^0E (Reijers *et al*., 1996). It is the youngest sedimentary basin in the Benue trough system. Figure 1 presents the study area: Eta (η) with Benin Flank by the zone; Calabar Flank (Murat, 1972). The study area has an abundant sequence of Neogene-Quaternary deposits. Akata-Agbada formations classify oil in this basin (Ekweozor & Daukoru, 1994; Tuttle, *et al*., 1999). The Akata formation is composed largely of marine shales and has an estimated thickness of up to 7 km (Doust & Omatsola, 1990). The Agbada formation is the core oil reservoir in the region. The Benin zone width is about 0.28 km but may be up to 2.1 km where it is extreme settling (Whiteman, 1982). The grain-particles of these rocks are identified due to their shapes, sizes, mineral structures, the age and time of deposition (Short & Stauble, 1967; Plummer & McGreary, 1993; Tamunobereton-ari *et al*., 2011). Niger Delta experiences wet season within the month of March and October as well as dry season within the month of November and February; average rain in a month during wet season is about 135 mm falling to 65 mm during dry season (Atat *et al*., 2012).

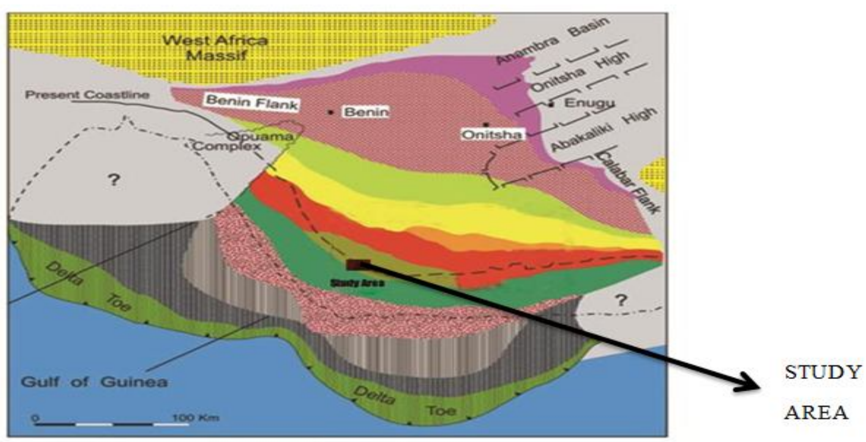

Figure 1: Map of Location of Study (Murat, 1972).

METHODOLOGY

The main software used for data processing and analysis is Hampson Russell. Two wells (G and H) were considered for this research. The data obtained include suites of log (Figure 2 and 3), Marker and 3D seismic (4 and 5). These data defined oilfield in the Niger Delta region.

We conditioned the logs, carried out analysis and enable the marker to map out the top and base of horizon and others. Seismic data was processed to transform seismic reflection data into a quantitative rock property description of the reservoir. The Seismic data has a dominant frequency of 60Hz. Inline from 4503 – 5563; Cross line 1540 - 2028 per the volume ranging from

350 to 5200ms. The seismic section has a sequence of parallel images offset and distorted by major average faults. Main counter faults are obvious in the cross mark segment via the volume and distorted peak and move above faults marked in the inline segment via the volume making it possible for normal faults to be sketched. Figure 6 is the base map for the three wells location. Figures 4 and 5 show the cross section of 3D full stack seismic information.

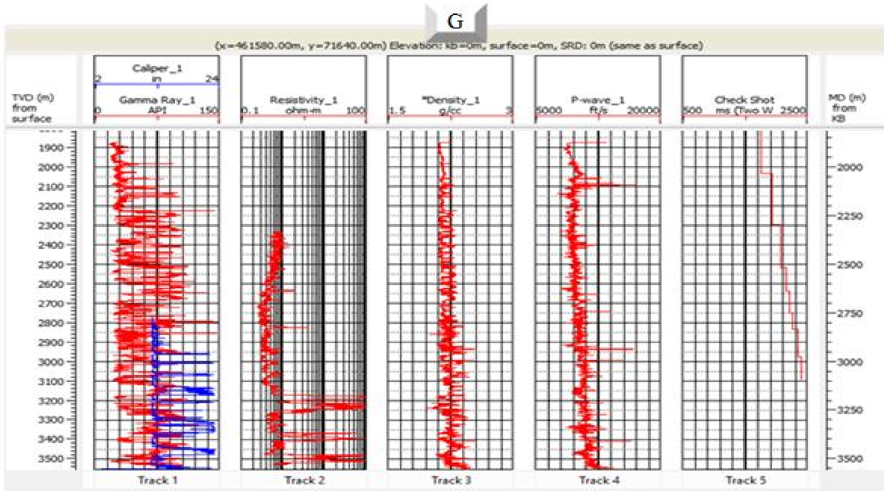

Figure 2: Suite of imported logs for Well G showing log signatures of Gamma ray, Resistivity, Density and P-wave.

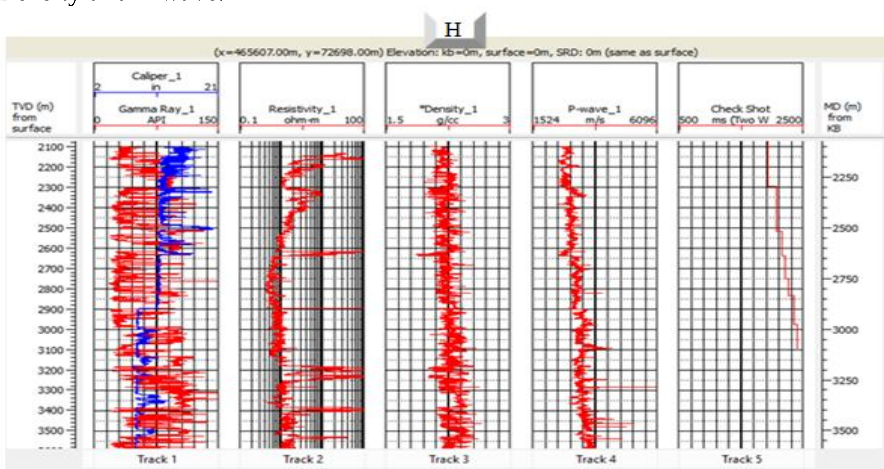

Figure 3: Suite of imported logs for Well H showing log signatures of Caliper, Gamma ray, Resistivity, Density and P-wave.

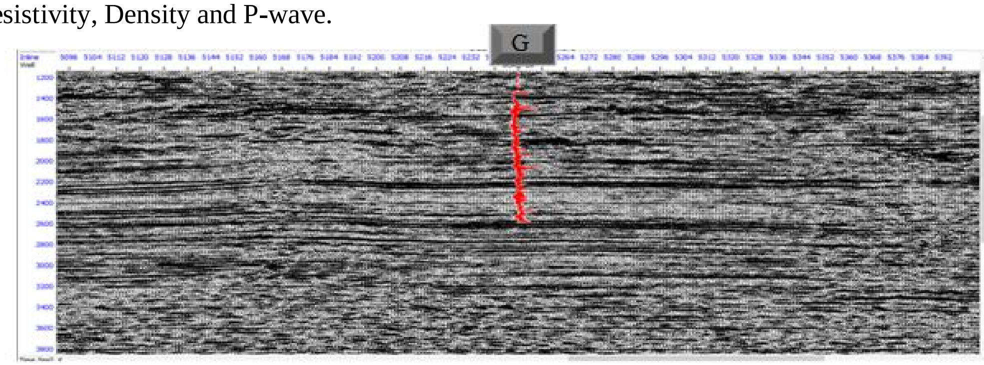

Figure 4: Inline and Crossline baseline seismic section η field between 1200-3800ms showing P-wave log at Well G.

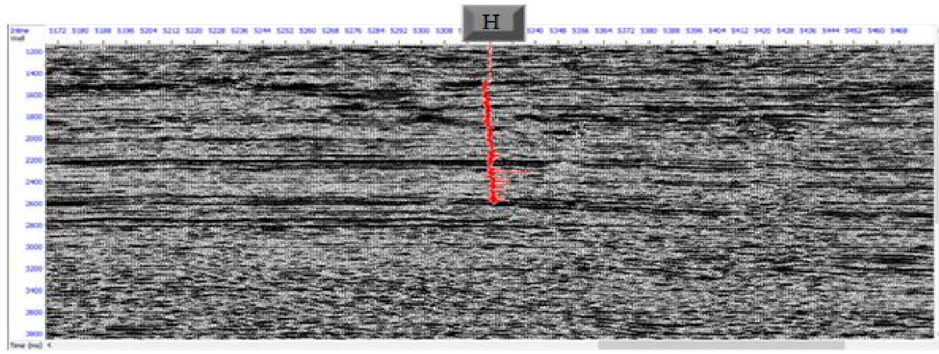

Figure 5: Inline and Crossline baseline seismic section η field between 1200-3800ms showing P-wave log at Well H.

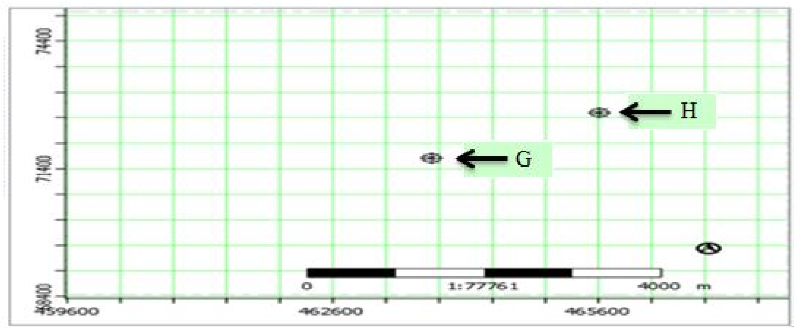

Figure 6: The 3D view base map of the wells locations in the η field. Two wells (G and H) imported shown in the base map are located at the north-east section of the field with their respective X and Y positions in metres.

Wavelet extraction is necessary for seismic inversion analysis. A reflection coefficient series from a well within the boundaries of the seismic survey is used to estimate accurate wavelet phase and frequency. Wavelet amplitude and phase spectra are estimated statistically from a combination of seismic data and well data using sonic and density curves.

To obtain seismic data, a survey was carried out by firing a short at the surface; it travels to the subsurface and the time was measured for the acoustic energy to travel down to a reflection surface and back up to the receiver surface. This information acquired, leads to seismic data. To obtain well log data, measurement were made relative to a device on the drill rig called the Kelly Bushing (KB) and differentiated between measured depth and true vertical depth since the depth is not purely vertical (Atat, *et al.*, 2020).

We used Hampson Russell software to process the data and estimate the pulse for a given window of real seismic data. This window was at the well location of interest. There are three pulse shapes: Minimum phase (wavelet starts at the position of the reflection coefficient; Zero phase (wavelet is centered on the reflection coefficient) and Quadrature phase (this is the zero phase pulse shifted by 90^0). Since seismic pulse changes in the earth due to attenuation; more synthetics based on different estimated pulse were generated, one for shallow target, another for intermediate target and lastly for deep targets. The wavelet converges more quickly than when starting with a zero phase assumption. We applied minor edits; stretch and squeeze to the data to align the seismic and well log reflectors better. Once the wavelet was identified, a synthetic seismic trace was computed for well log to original seismic correlation.

Well-to-seismic tie correlation rate depends on the quality of the well and seismic data and the time-depth relationship. The process was handled using Figure 7.

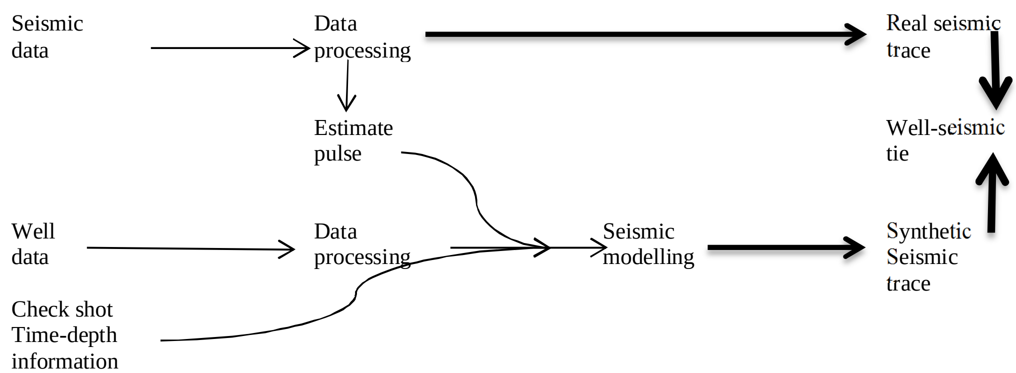

Figure 7: Well-to-Seismic Tie workflow

We edited the original sonic and density well-log of the two wells to remove spurious values using log math option to obtain filtered logs. Synthetic seismograms (trace) were generated from original sonic and density well log after the removal of spurious values; multiply sonic and density logs to have impedance logs as stated before. We converted well data in unit of depth to unit of time using check shot calibrated in time-depth curve for proper placement of the wells at their appropriate depths and time positions; the wavelet must tie the phase and frequency of seismic information. Well to seismic tie was established in time using statistical wavelet extracted from the data. With impedance, we calculated the reflection factors (coefficients); defined pulse removed. The reflection coefficient sequence is matched with the pulse to develop distinct wavelets to have synthetic trace. It is easier to interpret in the impedance domain than seismic domain since acoustic impedance relates with lithology.

RESULTS AND DISCUSSION

The best approach to relate the seismic response to rock properties using synthetic seismograms generated from well logs is the well-to-seismic tie. It enables the correct identification of mapped seismic reflections and made possible the connection among the impedance model and seismic statistics. This cannot be done without wavelet extraction that is most suitable for η-field. We extracted a wavelet from the data that increases the correlation between synthetics and the seismic data. This allows well facts noted in unit of penetration be equated to seismic records in unit of duration. The purpose is to obtain a wavelet character match and aids interpretation of the subsurface. The step-by-step result of this work is as presented in Figures 8 to 16.

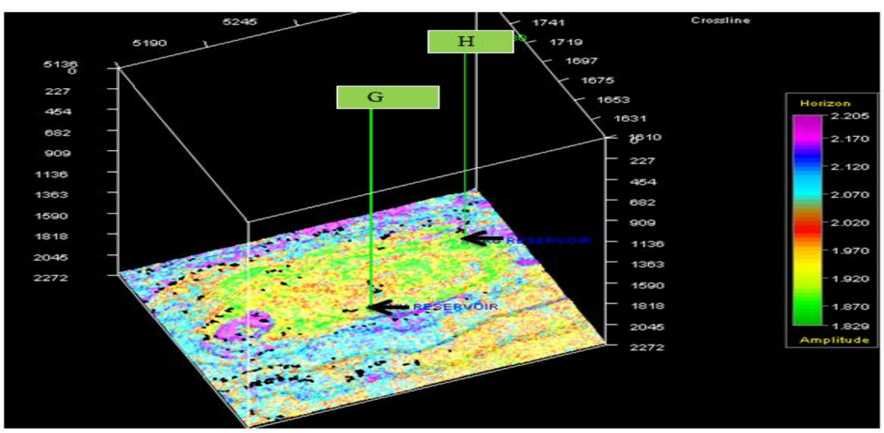

Figure 8: 3-D presentation of Well G and H Reservoirs.

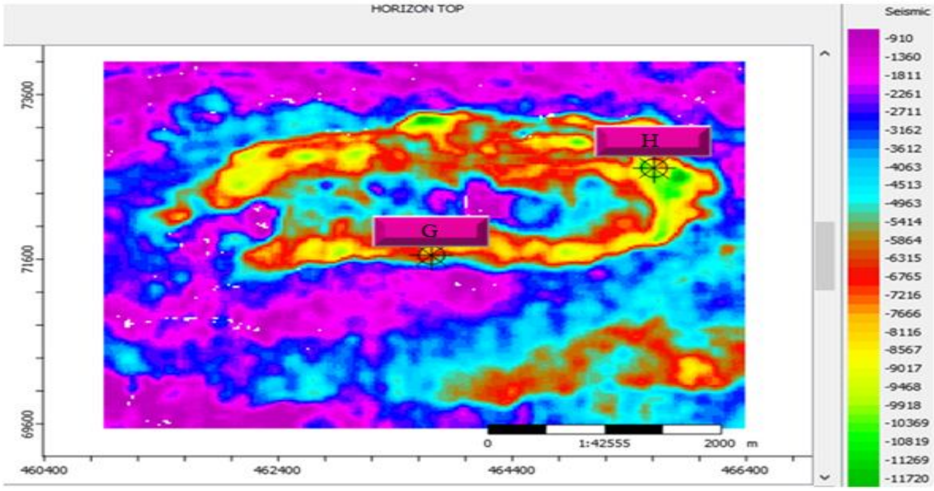

Figure 9: Top of horizon

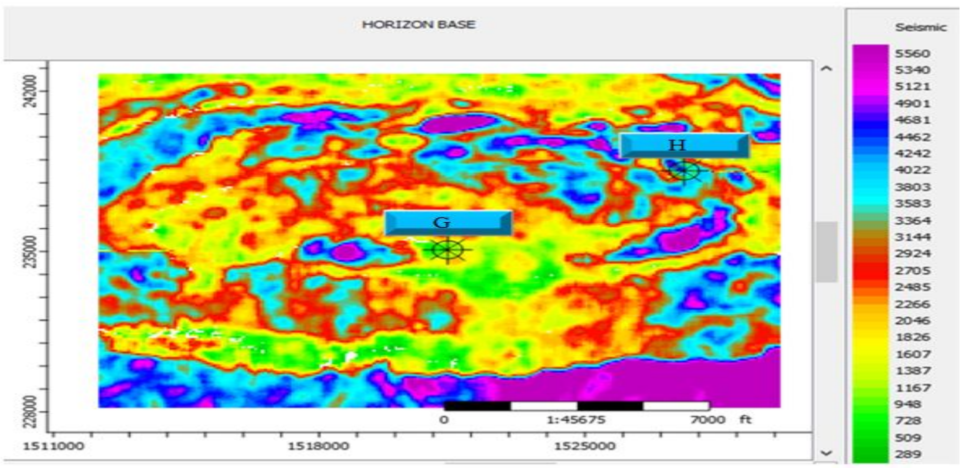

Figure 10: Horizon base

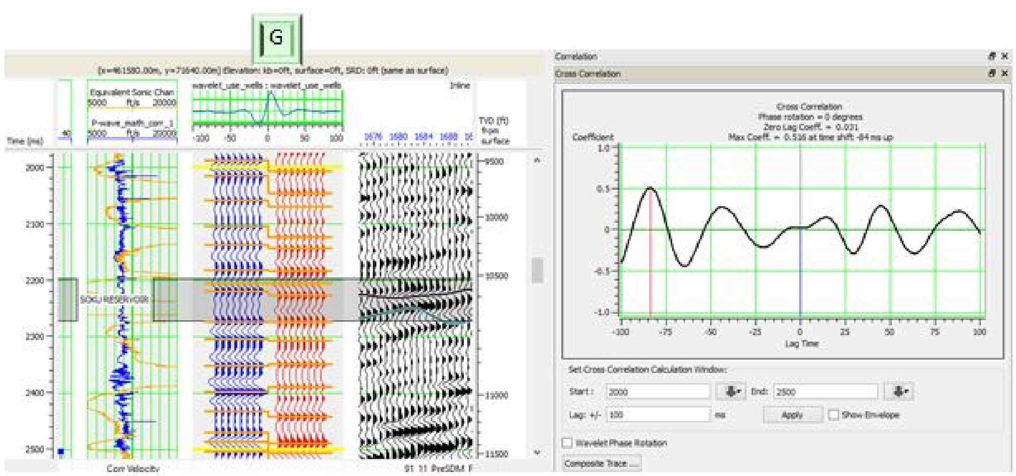

Figure 11: Statistically extracted wavelet used for well correlation by stretching and squeezing technique resulting in crosscorrelation plot of time shift -84ms up with correlation coefficient of <51% (right).

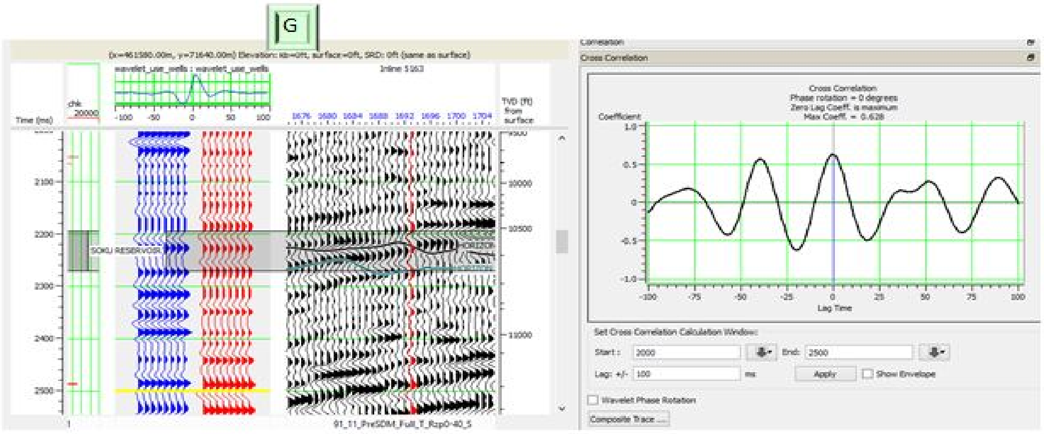

Figure 12: Re-extracted well option wavelet used for well correlation by stretching and squeezing technique leading to the crosscorrelation plot of time shift 0ms and correlation coefficient of >60% (right)

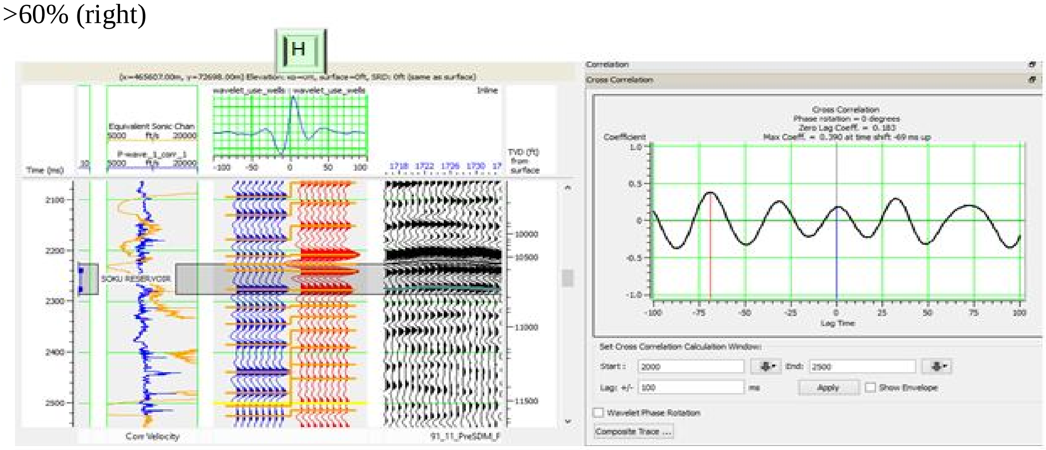

Figure 13: Statistically extracted wavelet used for well correlation by stretching and squeezing technique resulting in crosscorrelation plot of time shift -69ms up and correlation coefficient of <18% (right).

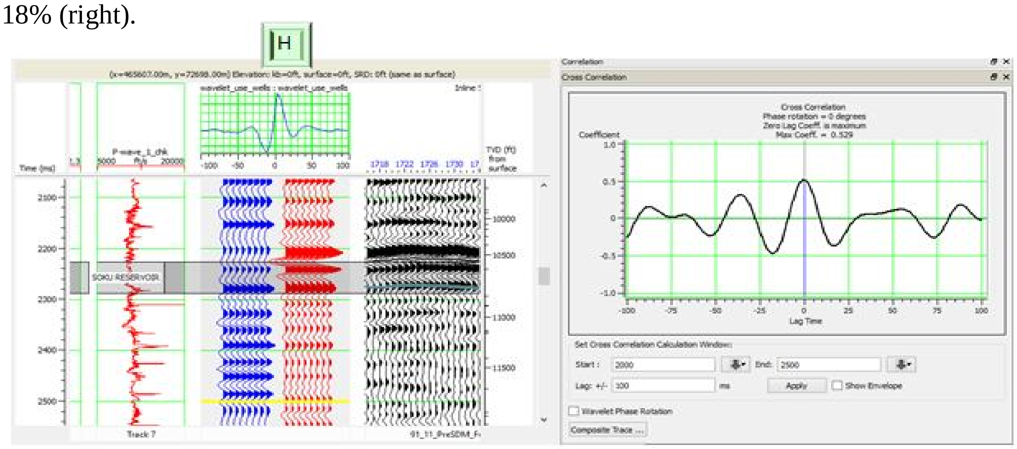

Figure 14: Re-extracted well option wavelet used for well correlation by stretching and squeezing technique leading to the crosscorrelation plot of time shift 0ms and correlation coefficient of 53% (right).

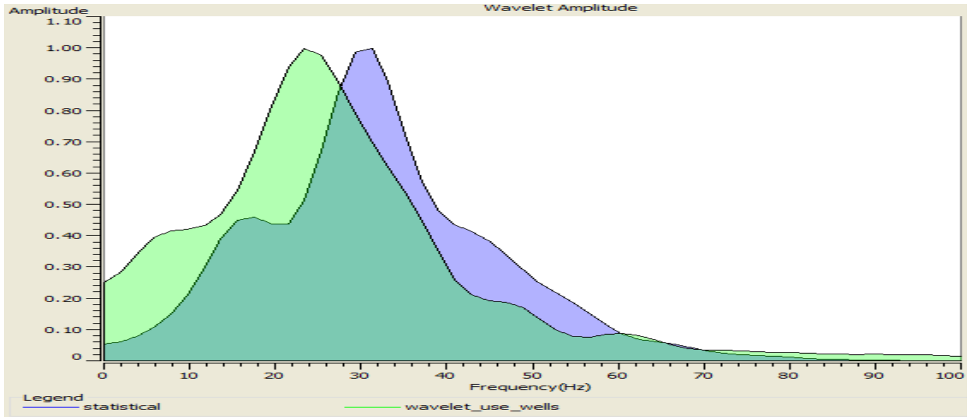

Figure 15: Amplitude spectrum of statistical (blue) and re-extracted (green) wavelets

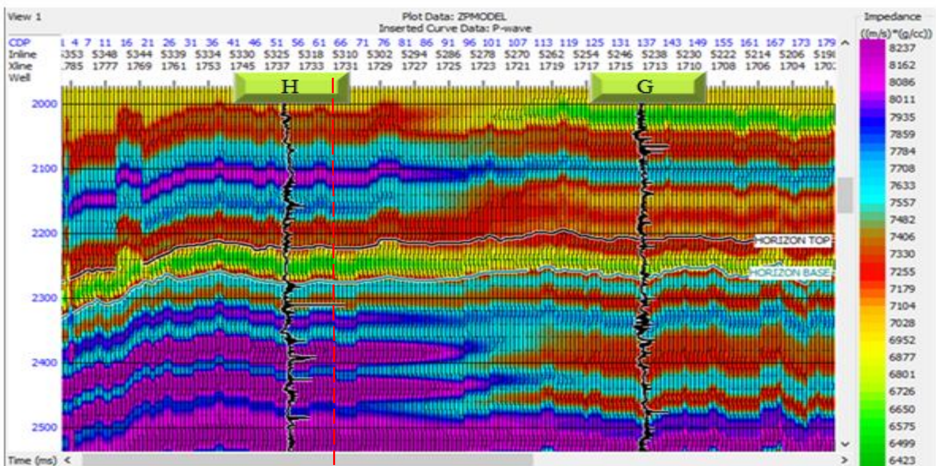

Figure 16: Inline/Xline arbitrary view of seismic section superimposed with colour section (initial model P -impedance) between 2000-2500ms showing P-wave log plot at Well G and Well H. Picked Horizons across the top and base of Reservoir expected where low P-Impedance log is bounded by low section of initial model

DISCUSSION

With the Marker, we were able to achieved Figures 8, 9 and 10 using Hampson Russell software. In the present work, we picked two main horizons using the stratigraphic control: horizon top and horizon base (Figures 9, 10 and 16). These horizons correspond to the main regional stratigraphic units in the study area. The horizon top (black marker) corresponds to the top of η formation, composed of negatively increased amplitudes to less negative amplitudes as shown in the color key (Figure 9). The lower cyan Marker (horizon base) is composed of positive amplitudes with sands over flooding the section (Figure 10).

We extracted the wavelet using a 400ms window centered between 2200 – 2600ms with its spectrum and the mis-match among the synthetic and seismic extraction. The synthetics were calculated by convolving the extracted wavelet (statistically) with impedance figured from the available well records. Statistically extracted wavelet used for well correlation by stretching and squeezing technique resulting in crosscorrelation plot of time shift -84ms up with correlation coefficient of <51% (Figure 11) and crosscorrelation plot of time shift -69ms up with correlation coefficient of <18% (Figure 13). This 18-51% mis-match with -69 to -84ms time lag between the seismic and synthetic data may be due to two reasons like no defined correlation window and bulk shift not yet applied.

Re-extracted well option wavelet used for well correlation by stretching and squeezing technique leading to the crosscorrelation plot of time shift 0ms and correlation coefficient of >60% (Figure 12) and the crosscorrelation plot of time shift 0ms and correlation coefficient of 53% (Figure 14). With the same time window of the wavelet estimation, correlation was done. The correlation coefficient improved to 53- 63% with 0ms time lag in Figures 12 and 14 when peak to peak on both synthetic and composite traces were manually aligned and wavelet re-extracted using well option. In particular, this re-extracted wavelet (Figure 15) was used for inversion of acoustic impedance yielding Figure 16. We filtered the acoustic impedance in 0.0 – 25.0Hz frequency series and interpolated the filtered result in the picked limits with exact stratigraphic switch using the inverse distance-based algorithm. This yields a detailed low-frequency model. This model contains information on the low-frequency trend that is unavailable in seismic amplitude information. Since seismic data is band limited (loss of low frequency content < 10Hz). What replaces this is the re-extracted wavelet from the wells.

CONCLUSION

We have considered researching on Attribute of influence of wavelet extraction on well-to-seismic tie in the η-Field. Seismic inversion analysis is always performed to have a better interpretation of seismic data as this increases efficiency and quality to improve assessment of rock properties. To achieve this, well-to-seismic tie which allows well data noted in unit of depth be matched to seismic facts in unit of time, was conducted were wavelet was extracted from seismic data using Hampson Russell software; impedance obtained from sonic and density logs and check-shots corrections applied. This is because impedance is a property of lithology and it is easier to interpret in impedance domain than seismic domain.

Statistically extracted wavelet used for well correlation resulting in crosscorrelation plot of time shift -84ms up with correlation coefficient of <51% and -69ms up with correlation coefficient of <18%. Re-extracted well option wavelet used for well correlation leads to a plot of time shift 0ms and correlation coefficient of >60% (well G); 53% for well H with the same time window of the wavelet estimation.

REFERENCES

Atat, J. G., Uko, E. D., Tamunobereton-ari, I. and Eze, C. L. (2020). Site-Dependent Geological Model for Density Estimation in the Niger Delta Basin, Nigeria. *Malaysian Journal of Geosciences*, 4(1): 1 – 6.

Atat, J. G., Akpabio, G. T. George, N. J. and Umoren, E. B. (2012). Geophysical Assessment of Elastic Constants of Top Soil using Seismic Refraction Compressional and Shear Wave Velocities in the Eastern Niger Delta, Nigeria. *International Journal of Modern Applied Physics*, 1(1): 7 – 19.

Doust, H. & Omatsola, E. (1990). Niger Delta. In: Edwards, J. D. & Santogrossi, P. A. Editions. Divergent/Passive Margin Basins. *American Association of Petroleum Geologists Memoir 48*. Tulsa: American Association of Petroleum Geologists. pp. 239 – 248.

Ekweozor, C. M. & Daukoru, E. M. (1994). Northern Delta Depobelt Portion of the Akata-Agbada Petroleum System, Niger Delta, Nigeria. In: Magoon, L. B. & Dow, W. G. Editions. The Petroleum System from Source to Trap. *American Association of Petroleum Geologists Memoir 60*. Tulsa: American Association of Petroleum Geologists, pp. 599 – 614.

Geo, J., Zhang, B., Han, W., Peng, J. and Xu, Z. (2017). A New Approach for Extracting the Amplitude Spectrum of the Seismic Wavelet from the Seismic Traces. *IOP Inverse Problem*, 13: 1 – 6.

Klett, T. R., Ahlbrandt, T. S., Schmoker, J. W. and Dolton, J. L. (1997). Ranking of the World's Oil and Gas Provinces by Known Petroleum Volumes. *United State Geological Survey Open-File Report*, 97, 463.

Margrave, G. F. (1998). Theory of Non-Stationary Linear Filtering in the Fourier Domain with Application to Time-Variant Filtering. *Geophysics*, 63(1): 244 – 259.

Margrave, G. F. and Lamoureux, M. P. (2001). Gabor Deconvolution. *CREWES Research Report*, 13: 241 – 276.

Murat, R. C. (1972). Stratigraphy and Paleogeography of the Cretaceous and Lower Tertiary in Southern Nigeria. In Dessauvagie, T. F. G. & Whitman, A. J. eds., *African Geology*. Ibadan: University of Ibadan Press. Pp 251 – 266.

Plummer, C. C. and McGreary, D. (1993). *Physical Geology*. 6th Edition. England: Wm. C. Brown Publishers.

Reijers, T. J. A., Petter, S. W. and Nwajide, C. S. (1996). The Niger Delta basin: Reijers, T.J.A., ed., Selected Chapter on Geology: SPDC Wa.: LP1O3-118.

Robinson, E. A. and Treitel, S. (2000). *Geophysical Signal Analysis*. Tulsa: Society of Exploration Geophysicists.

Short, K. C. and Stauble, A. J. (1967). Outline of Geology of the Niger Delta. *Journal of the American Association of Petrololeum Geologists*, 51(5): 761 – 799.

Schlumberger Limited (2020). Oilfield Glossary.

Tamunobereton-ari, I., Omubo-Pepple, V. B. and Uko, E. D. (2011). Determination of the Variability of Seismic Velocity with Lithology in the Southwestern Part of the Niger Delta Basin of Nigeria Well Logs. *Journal of Basic and Applied Scientific Research*, 1(7): 700 – 705.

Tan, T. H. (1999). Wavelet Spectrum Estimation. *Geophysics*, 64: 1836 – 1846.

Tuttle, M. L. W., Charpentier, R. R. and Brownfield, M. E. (1999). The Niger Delta Province, Nigeria, Cameroon and Equatorial Guinea, Africa.

Wang, X., Xiao, Q., Xia, C., Wu, Z. and Xie, C. (2017). Far-Field Wavelet Extraction and Application of Vertical Cable System. *Journal of Pure and Applied Geophysics*, 174: 1779 – 1786.

Weglein, A. B. and Secrest, B. G. (1990). Wavelet Estimation for a Multidimensional Acoustic or Elastic Earth. *Geophysics*, 55: 902 – 913.

Wei, F., Tian-Yue, H., Feng-Chang, Y., Yan, Z., Yong-Fu, C. and Geng-Xin, P. (2017). Time-Varying Seismic Wavelet Estimation from Non-Stationary Seismic Data. *Chinese Journal of Geophysics*, 60(2): 191 – 202.

Whiteman, A. (1982). *Nigeria: Its Petroleum Geology, Resources and Potential*. London: Graham and Trotman.

Yi, B., Lee, G., Kim, H., Jou, H., Yoo, D., Ryu, B. and Lee, K. (2013). Comparison of Wavelet Estimation Methods. *Geosciences Journal*, 17 (1): 55 – 63.

Zang, P., Dai, Y., Tan, Y., Zhang, H. and Wang, C. (2018). A Time-Varying Wavelet Phase Extraction Method using the Wavelet Amplitude Spectra. *System Science and Control Engineering*, 6(3): 10 – 18.